

Three upgrade scenarios for PIAVE-ALPI complex are foreseen, with an increase of final energy and beam quality as a result. The upgrades are organized in stages following a costs optimization criterion, which means that the specifications for new equipments are given keeping in mind the final stage. Hence the intermediate solutions do not waste previous capital investments.

The first scenario is called AGATA, its specifications derive from the present limits of PIAVE-ALPI accelerator complex and its aim is to fulfill the AGATA user groups requests. The last scenario is called SPES and it implies a radical change in PIAVE layout and in the overall ALPI performances in view of the acceleration of Radioactive Ion Beams. It needs a full funding support and it represents the maximum exploit of ALPI accelerating structures. The intermediate scenario, "intermezzo", gives the chance to get a substantial improvement of AGATA scenario with little financial effort.

## 5.1 Preliminary considerations

As described in Chapter 1, ALPI accelerator hardware choices come from late 80's. The main characteristics of ALPI from the beam dynamics point of view are the available cavity maximum accelerating fields and the magnets maximum gradient. If the former are being continuously enhanced, the latter can be increased only buying completely new hardware. Given the near future expected cavity performances, new beam dynamics choices have to be made to design a transport which fully exploits the higher accelerator gradient.

The scenarios main features are reported in Fig. 5.1 and the details are discussed hereafter.

### Cavity accelerating fields

- *Low- $\beta$  cavities.* If operated at  $E_{acc} > 3.5$  MV/m a cooling system for the RF coupler and a new bottom tuner plate are required [1]. The CR03 cryostat comprises these improvements and the expected  $E_{acc}$  for 2009 is 5 MV/m. In few years all the low- $\beta$  cryostats and cavities will be upgraded and  $E_{acc}$  will reach 6 MV/m.
- *Medium- $\beta$  cavities.* The performances of the medium- $\beta$  cavities installed in ALPI have improved year by year. The last release of the inner structure (beam ports and stem) and accurate polishing techniques allow to use them safely at 4.5 MV/m [2]. Therefore an average  $E_{acc}$  of 4.2 MV/m is foreseen for 2009 (and hence for AGATA scenario) and once the upgrade program is completed, it will be possible to reach an average  $E_{acc}$  of 4.5 MV/m.
- *High- $\beta$  cavities.* The high- $\beta$  cavities work at 5.5 MV/m flawlessly.

### Magnets

As explained in Section 1.3, the increased equivalent voltage of the accelerator could be supported by a proper beam dynamics only if the longitudinal phase amplitude oscillation are damped (i.e.

Table 5.1: PIAVE-ALPI hardware performances for the upgrade scenarios.

parameter	# of cav.	present	AGATA	"intermezzo"	SPES opt. I	SPES opt. II
<i>low-beta (<math>\beta_o = 0.047</math> and <math>\beta_o = 0.056</math>), 80 MHz</i>						
CR01-02	8	n/a	n/a	n/a	6	n/a
CR03	4	n/a	5	6	6	6
CR04-06	12	3.5	3.5	6	6	6
<i>medium-beta (<math>\beta_o = 0.11</math>), 160 MHz</i>						
CR07-18	44	4.2	4.2	4.5	4.5	4.5
<i>high-beta (<math>\beta_o = 0.13</math>), 160 MHz</i>						
CR19-20	8	5.5	5.5	5.5	5.5	5.5
CR21	4	n/a	n/a	n/a	5.5	5.5
CR22-23	8	n/a	n/a	n/a	n/a	5.5
total cavities		64	68	72	80	80
triplet max gradient		20 T/m		30 T/m		
# above 21 T/m		0	0	4	12 (14)	9
long. dynamics		present		new buncher	new buncher + new injector	

the longitudinal phase advance is reduced), that implies the use of alternating synchronous phases. Therefore the RF defocusing acts asymmetrically respect to the period center and the transverse envelope is kept limited (along with the emittance growth) only if a proper choice of the accelerating field is made. Summing up, the higher is the field the higher is the number of the positive synch. phases to be used and the more uneven is the transverse envelope.

The solution is to squeeze the beam as much as possible implying high performances for the triplets, beyond the limits of the present ones (max. nominal gradient 20 T/m). Therefore for the more demanding scenarios some new triplets will be required (max. nominal gradient 30 T/m). In Tab. 5.1 a line with the number of triplets beyond the limit of 21 T/m is reported <sup>1</sup>.

### Implications of longitudinal beam dynamics

The critical part of the acceleration set-up in ALPI, as described in Chapter 1, is the longitudinal emittance out of PIAVE and a proper longitudinal focusing to the first low- $\beta$  cryostat. The solution found in the last shifts (2007/2008) foresees CR04 as buncher cryostat, where large synchronous phases and reduced  $E_{acc}$  are used. This costs  $\sim 2$  MV of low- $\beta$  acceleration and even more taking into account the low TTF in the first medium- $\beta$  cavities. A new super-conducting buncher would be advisable to obtain the requested focusing at ALPI beginning and a new PIAVE layout is needed in order to have a lower longitudinal emittance. Combined, it results that a narrower acceptance could be sustained and higher acceleration becomes possible.

## 5.2 AGATA scenario

As reported in Tab. 5.1, a new low- $\beta$  cryostat will be available in ALPI in autumn 2008. CR03 cryostat completes the first ALPI period (see FIG. 5.2(a)) and it will gently focus the beam to the

<sup>1</sup>21 T/m is the value which is considered the actual limit for such magnets.

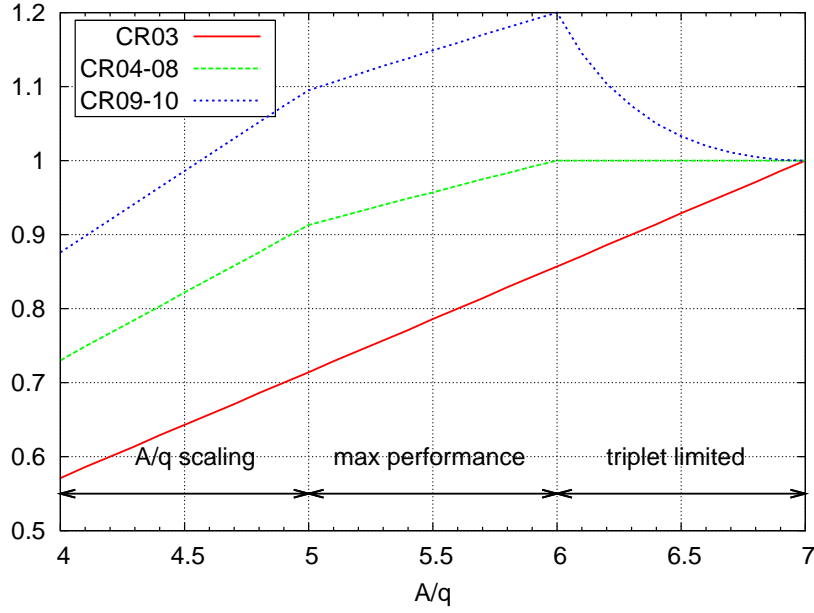


Figure 5.1: ALPI low-energy branch QWR accelerating field scaling law for AGATA scenario with respect to  $A/q = 7$ . For  $6 \leq A/q \leq 7$  the  $E_{acc}$  of CR09-10 values can be raised since the beam dynamics is dominated by the 3Q5 maximum gradient (20 T/m).

following cryostat, taking the role which CR04 has in the present beam dynamics. The normal-conducting buncher HEB-2 is unable to strongly focus the beam at CRO4 due to the too long distance between them and moving HEB-2 closer to CRO4 would require a  $E_{acc}$  beyond the limits of the cavity. The result is that only a small acceleration is given by CRO3 to the beam. The transverse envelopes along the period are yet smoother compared to the present beam dynamics and it easier to get the focus at the center of the period avoiding the risk of losing part of the beam onto the cavity beam ports.

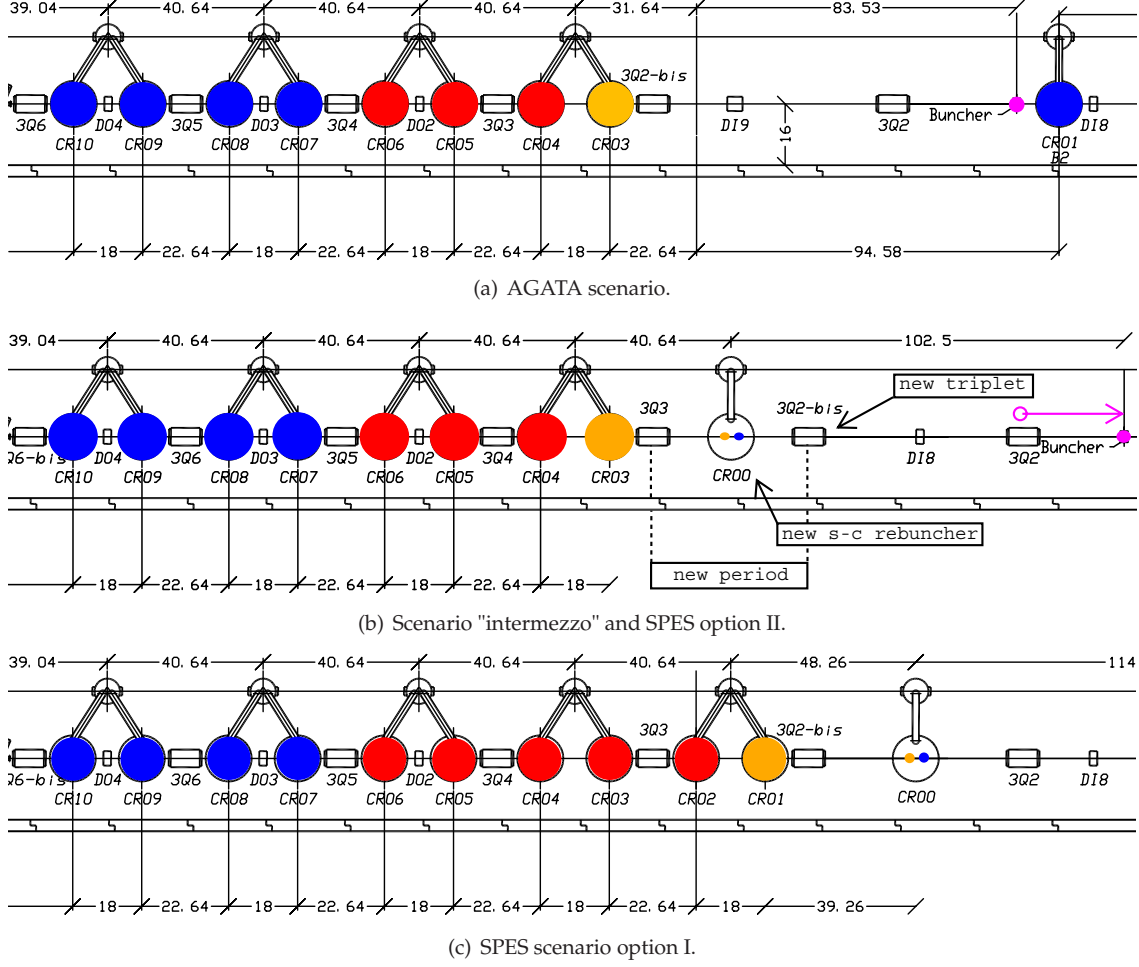
The  $E_{acc}$  values are chosen as function of the  $A/q$  in order to get the maximum energy minimizing losses and emittance growth (see Fig. 5.1).

- $6 \leq A/q \leq 7$ . The beam dynamics has been optimized for  $A/q = 7$ , having the maximum gradient of 3Q5 (the last triplet of the low-energy branch) as major limit. The  $E_{acc}$  of CR09 and CR10 can be raised for  $A/q < 7$  and the configuration of maximum field is obtained for  $A/q = 6$ .
- $5 < A/q < 6$ . The  $E_{acc}$  is decreased less than the linear  $A/q$  scaling because the longitudinal match can be found by switching the sign of specific synchronous phases.
- $4 \leq A/q \leq 5$ . The  $E_{acc}$  values scale as  $A/q$ . For  $A/q = 5$  the beam dynamics limit (longitudinal phase advance and RF defocusing) is reached.

In Fig. 5.3 three plots describe the cavities usage for this scenario. Looking at the TTF graph, it results that for  $A/q = 4$  the acceleration efficiency is at its maximum. In order to accelerate heavier ions more efficiently, more low- $\beta$  cavities are needed. The solution is to free CR03 cryostat from the bunching task and to add an 80 MHz buncher in front of the first ALPI period.

### 5.3 "Intermezzo" scenario

As reported in Tab. 5.1, all the low- $\beta$  cavities are expected to work at 6 MV/m. No restriction are made on the triplets, having in mind that this scenario is a preparatory stage to the final



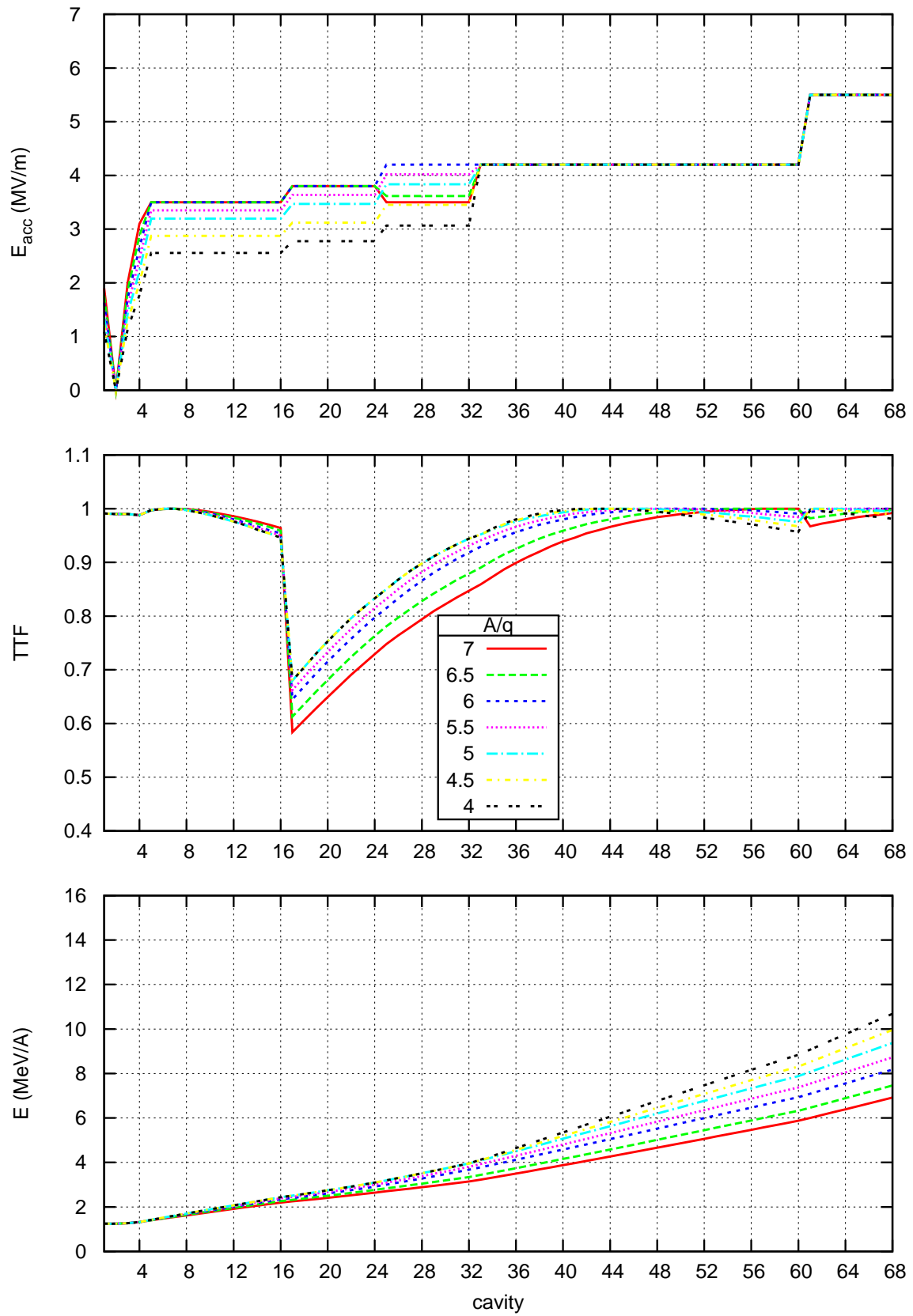


Figure 5.3: Performances of ALPI for AGATA scenario.

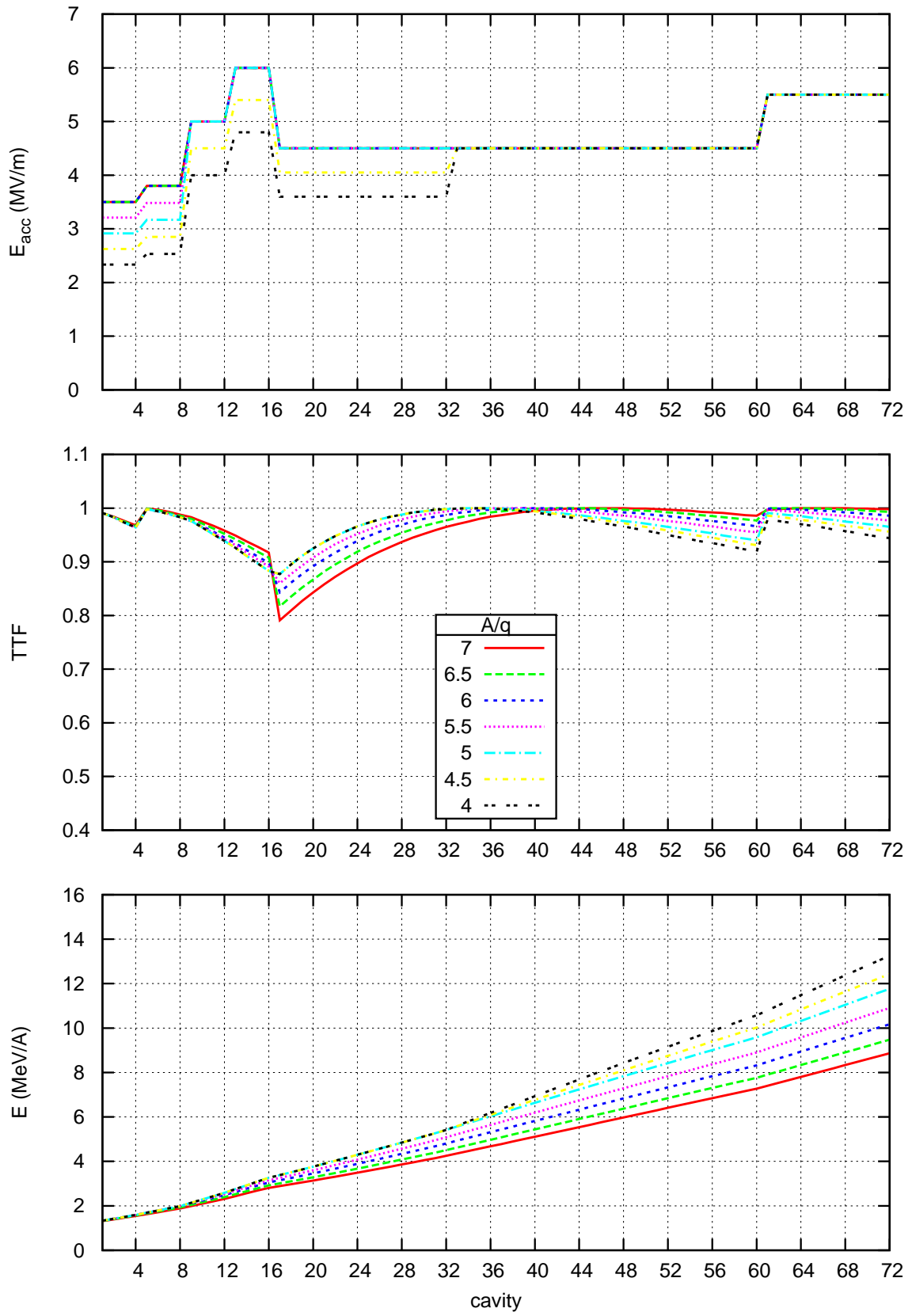


Figure 5.4: Performances of ALPI for scenario "intermezzo".

The new 80 MHz cavity before ALPI low-energy branch induces to develop a new small cryostat housing both the 80 and the 160 MHz buncher. The present CRB2 cryostat can be placed in the ALPI high-energy branch without modifications and it will complete ALPI last present period (CR20-CR21) increasing the high-energy branch voltage by about 4 MV.

## 5.4 SPES scenario

As said in Chapter 2, the weakness of PIAVE layout (see Fig. 5.6(a)) is the lack of a proper bunching section before the QWR cryostats. In the present set-up the first cavity is used as buncher, but this results in a residual longitudinal emittance increase. With such a longitudinal emittance the first part of the acceleration in ALPI is troublesome and longitudinal losses can not be avoided.

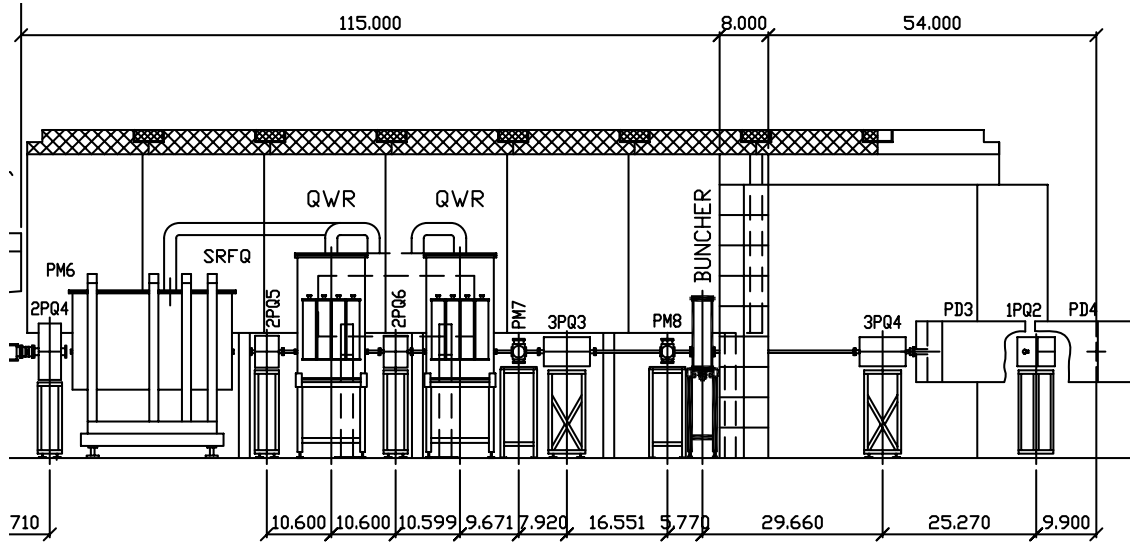
The second problem is the use of alternating synchronous phases with a transverse focalization given by a doublet focusing period. The result is that the beam has different envelopes for x and y plane, that causes different transverse emittance growth as reported in the second column of Tab. 5.2.

Concerning the diagnostics placement, the compactness of PIAVE layout, which in principle could have many advantages in shortening the transverse and longitudinal period (i.e. phase advance), is a serious problem. The first diagnostic box downstream the SRFQs is placed only after the two QWR cryostats. This means that, if during a shift unexpected beam losses are found along the line, it is not possible to distinguish whether the problem comes from the SRFQs or from the QWRs without switching off all the cavities and resetting the magnets. A proper and more comfortable diagnostics placement would be after the SRFQs to check the beam current and between the two cryostats to check if any loss occurs due to beam misalignment and cavity steering effect [3].

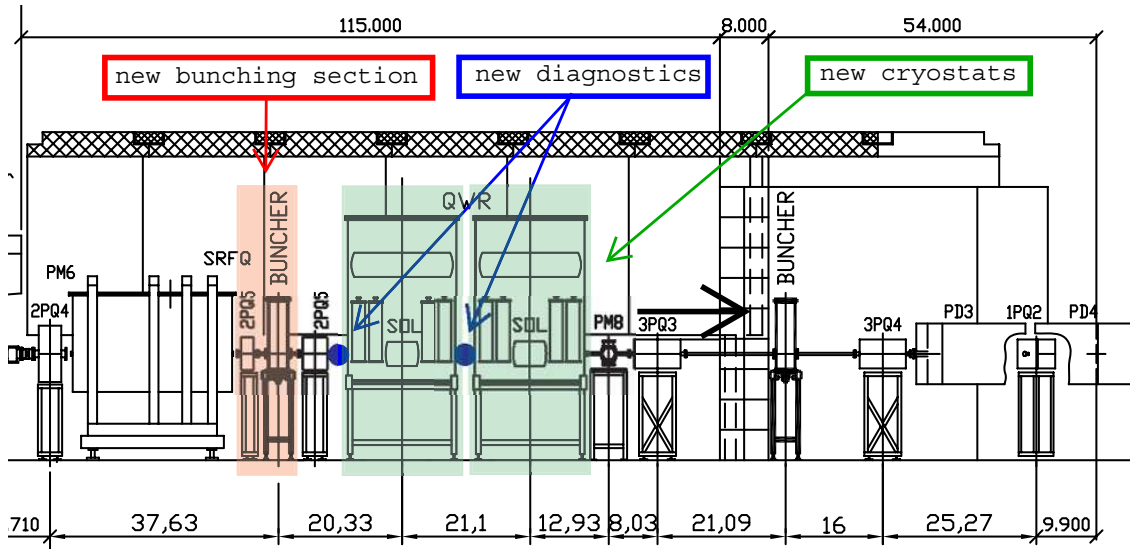
### 5.4.1 The new Piave layout

For the previous reasons a new layout (see Fig. 5.6(b)) of the line after the SRFQs is proposed hereafter. The only constraint is the available distance between the SRFQs and front shielding wall to ALPI common room.

- *Bunching section.* A new low-energy n-c buncher is foreseen. The buncher is made by modifying HEB2 [5] keeping the QWR resonant cavity and all the ancillaries (RF amplifier, electronics, cooling system, support) but changing the internal stem and gaps width. To take full advantage of the new buncher a thin ( $L_{eff} = 15.6$  cm) low gradient ( $\sim 13$  T/m for  $A/q = 7$ ) quadrupole is placed between the SRFQs and the buncher at the x-plane waist in order to reverse the transverse beam divergence without affecting the quadrupole symmetry. Therefore the transverse dimensions of the beam are equal inside the buncher. 2PQ5 doublet focuses the beam at the first QWR cavity and the round condition could be achieved setting appropriately the singlet field.
- *New cryostats.* The present PIAVE layout wastes the opportunity of high gradient beam dynamics because of the funnel-shaped use of the synchronous phases, where the  $E_{acc}$  is lowered to obtain a wider longitudinal acceptance. To overcome the problem a shorter longitudinal and transverse period could be designed. The best solution is a cryostat where the QWRs are housed together with a compact super-conducting solenoid. The cryostat looks very similar to the one already adopted at ISAC2 TRIUMF) [4] (see Fig. 5.7), which houses four 106 MHz QWR cavities and a s-c solenoid (max 9 T). The big advantage of this solution is that the distance between the two cavities facing the solenoid is very close to the one between the two cavities facing the space between cryostats. This means having a longitudinal period which is half the transverse period. From the point of view of transverse focusing, the solenoids give the unique opportunity of maintaining equal conditions for x and y plane and having a round beam along all the acceleration as a result. Moreover, between the cryostats a diagnostic box and a steerer is foreseen in addition to the space for



(a) PIAVE present layout.



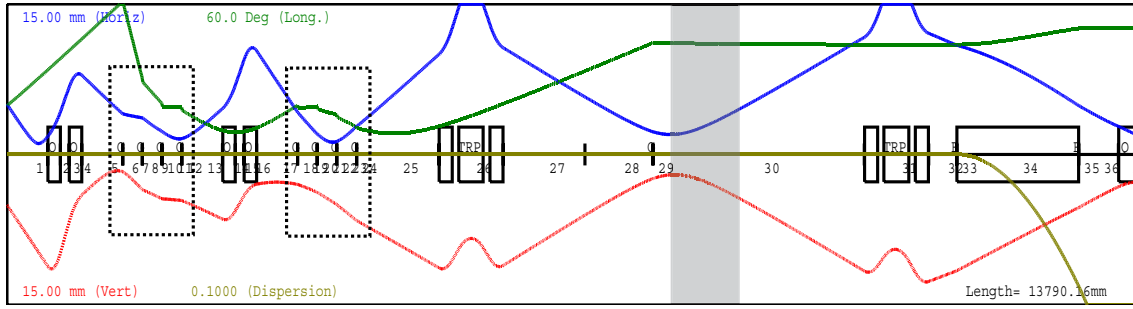
(b) PIAVE new layout.

Figure 5.5: PIAVE layout comparison. A magnetic singlet and a n-c 80 MHz buncher are installed in the new bunching section.

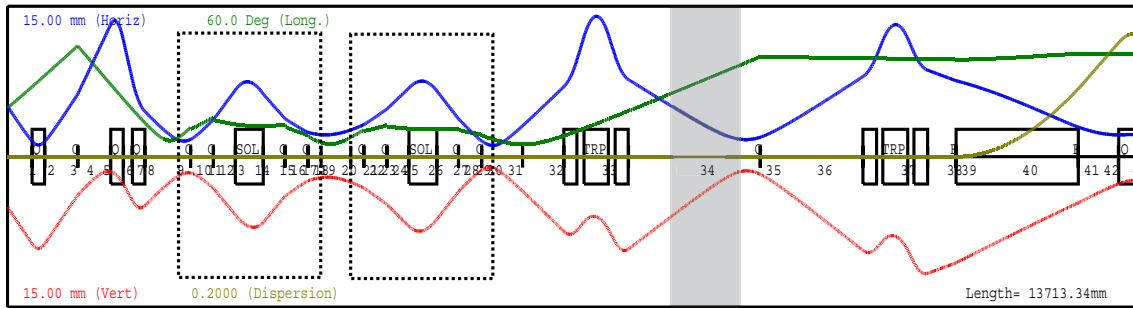
Table 5.2: Comparison between PIAVE present and new layout beam dynamics results.

	SRFQ out	present PIAVE	new PIAVE	unit	var.
$\epsilon_{x \text{ rms}}$	0.100	0.102	0.105	mm mrad n.	+3%
$\epsilon_{y \text{ rms}}$	0.100	0.133	0.105		-21%
$\epsilon_{z \text{ rms}}$	0.055	0.121	0.062		-49%
E	0.59	1.18	1.45	MeV/A	+23%





(a) PIAVE present layout.



(b) PIAVE new layout.

Figure 5.6: PIAVE beam dynamics comparison from the SRFQ output to the L-bend singlet. The dotted rectangles represent the cryostats and the grey band the shielding wall. Trace 3D envelopes.

Table 5.3: PIAVE beam dynamics comparison. The accelerating fields  $E_{acc}$  in [MV/m] are referred to the  $A/q = 7$  case and the energy  $E$  is expressed in [MeV/A].

QWR	present			new		
	$E_{acc}$	$\phi_s$	E	$E_{acc}$	$\phi_s$	E
low-energy buncher				0.91	-90	0.588
1.1	2.9	-90	0.588	3.50	-30	0.656
1.2	3.2	+60	0.623	4.85	-30	0.756
1.3	4.1	+30	0.706	5.25	-30	0.869
1.4	4.1	-25	0.797	5.25	-30	0.984
1.5	4.5	-20	0.891	5.25	-30	1.101
1.6	4.5	-20	0.987	5.25	-30	1.218
1.7	4.5	-20	1.084	5.25	-30	1.334
1.8	4.5	+20	1.180	5.25	-30	1.449

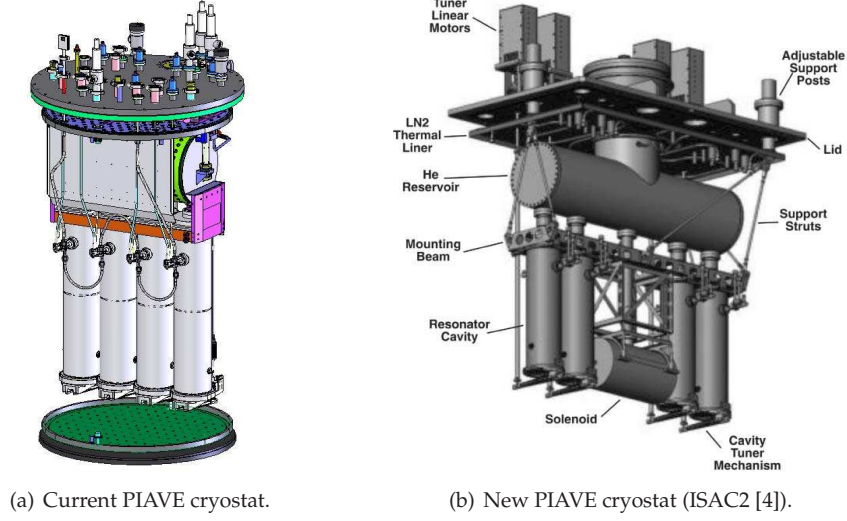


Figure 5.7: PIAVE cryostat comparison. ISAC2 cryostat houses four QWRs and a compact s-c solenoid (max 9 T).

Table 5.4: Beam dynamics results in case of a single cavity failure for the new PIAVE layout.

	<i>all</i>	1.1 off	1.2 off	1.3 off	1.4 off	2.1 off	2.2 off	2.3 off	2.4 off	unit
$\epsilon_{x \text{ rms}}$	0.105	0.105	0.105	0.100	0.104	0.101	0.100	0.103	0.103	mm mrad n.
$\epsilon_{y \text{ rms}}$	0.105	0.108	0.105	0.102	0.103	0.103	0.102	0.104	0.105	
$\epsilon_{z \text{ rms}}$	0.066	0.065	0.070	0.062	0.063	0.063	0.063	0.064	0.065	
E	1.45	1.37	1.31	1.35	1.36	1.34	1.34	1.33	1.31	MeV/A

the vacuum valve. This allows to check the transverse conditions between the two cryostats in the focal point of the solenoid as it happens in ALPI period (see Fig. 1.2) for triplets. This diagnostics box combined to the one placed after 2PQ5 will be used to check the correct transverse match parameters and in particular the roundness of the beam before entering the first cryostat.

- *New HEB-1 position.* Since the new bunching section is added and the new QWR cryostats are longer, HEB-1 buncher will be moved after the shielding wall in the room common to the injecting and extracting lines of ALPI and a proper shielding will be tailored around it.

In Table 5.2 the beam dynamics results of new layout are compared to the ones of the present layout. With the new layout a very low longitudinal emittance growth (10%) can be reached and the transverse emittance increase is limited to 5%, equal in the x and y plane as a consequence of the new roundness condition.

The further advantage of this solution is to operate the injector even with a single cavity failure, which was not possible to be performed in the present layout. Table 5.4 shows the results of a set of simulations which are carried out optimizing the output Twiss parameters, which means round beam and longitudinal parameters compatible to the parallel transport in the L-bend section. The results are quite encouraging because the output energy in all cases is higher than the reference output energy for present layout and the emittance growth is of the same order of magnitude of the new reference design. In most cases the asymmetry of the transverse emittance growth comes from a different focusing condition at the buncher location to ensure symmetric envelopes along the acceleration.

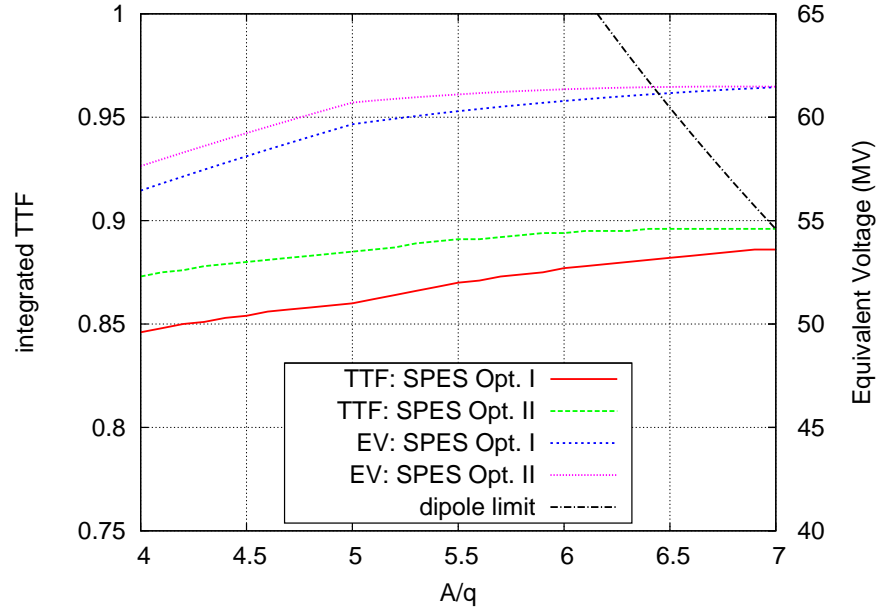


Figure 5.8: Comparison between two possible upgrade solutions for SPES scenario. Either the low-energy (CR01-02) or the high-energy branch (CR22-23) is upgraded.

### 5.4.2 ALPI upgrade

As a consequence of the new PIAVE layout two low- $\beta$  "traditional" cryostats become available in ALPI. This means that the ALPI low- $\beta$  or high- $\beta$  branch could be extended at the minor cost of 8 new QWRs and ancillaries (RF amplifiers, control electronics, vacuum system) and the link to the present cryogenic system which is under upgrading [6]. The cryostats, even if designed for 80 MHz QWRs, can be easily adapted to the 160 MHz QWRs.

- I *Low- $\beta$  upgrade.* The new period before CR03 can be filled with the two cryostats recovered from PIAVE and CR00 will be moved one period upstream. The last two low- $\beta$  cryostats can be required to work at  $E_{acc} = 6$  MV/m up to  $A/q = 5$ . This way, the acceleration efficiency would be favorable to the heaviest ions, whereas the lightest ones would suffer from an excess of low- $\beta$  cavities (see Fig. 5.8). However, this allows to transport the beam efficiently even if some low- $\beta$  cavities were out of order. To enhance the overall efficiency of the low- $\beta$  section for the lightest ions, a solution could be found by changing the optimum beta of the QWR installed in CR05-06 ( $\beta_o = 0.056$ ) to a higher value ( $\beta_o \approx 0.07$ ). This means that the QWRs of CR05-06 are removed from these cryostats and installed in CR02-03, and the present cavities of CR03 will be moved to CR01.
- II *High- $\beta$  upgrade.* The second solution is to place the two cryostats downstream the high-energy branch. This way the number of cavities is divided among the three optimum beta so to keep the performances of Option II for the heaviest ions and to enhance the final energy for the lightest (see Fig. 5.10). The low- $\beta$  upgrade can be performed later on.

In both cases the maximum energy can not be reached for ions with  $A/q > 6.4$ . This is due to the maximum magnetic field of the dipoles (1.6 T) (see Fig. 5.8) and it would cost up to 1 MeV/A for  $A/q = 7$ .

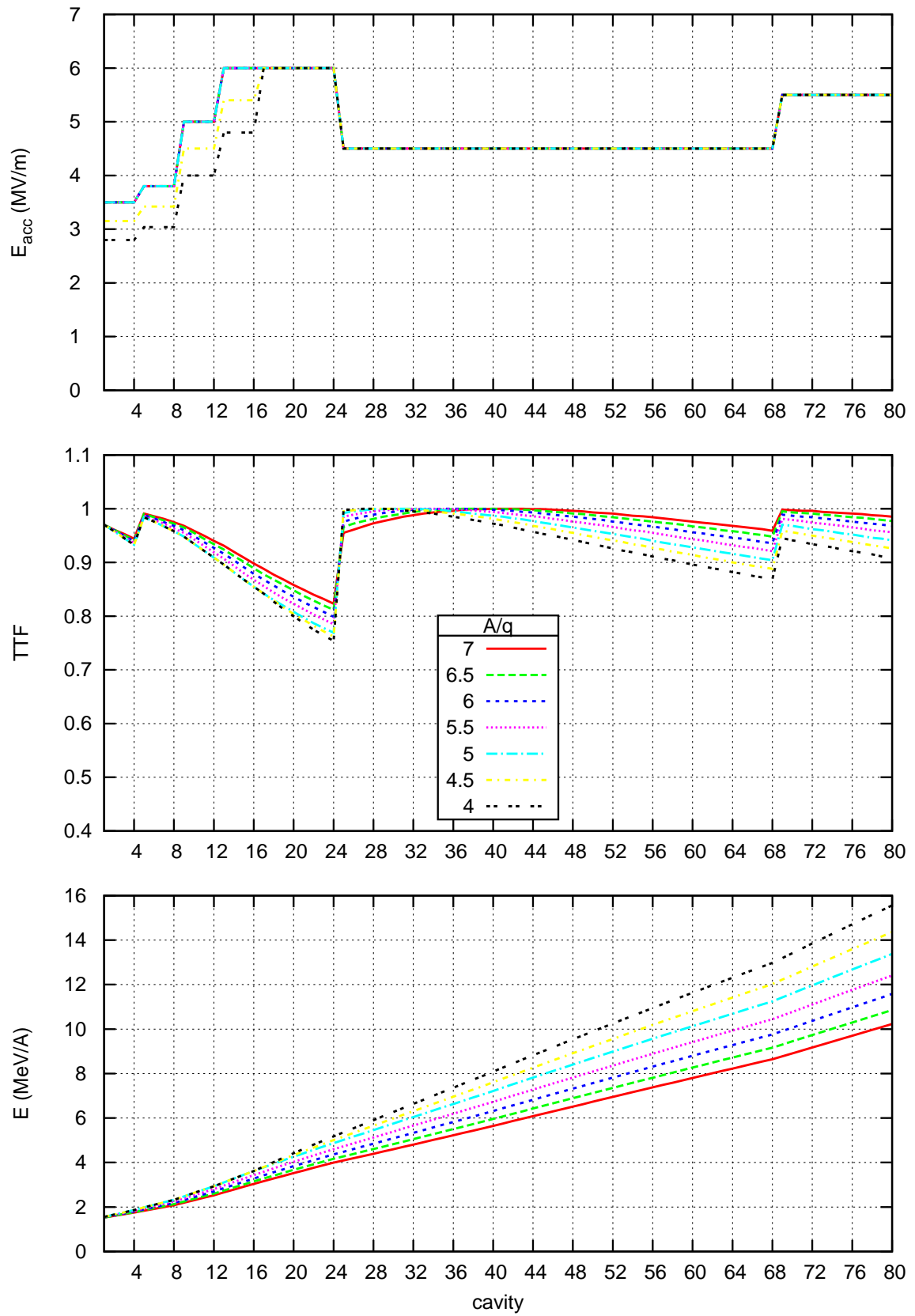


Figure 5.9: Performances of ALPI for SPES scenario. Option I, low-beta upgrade.

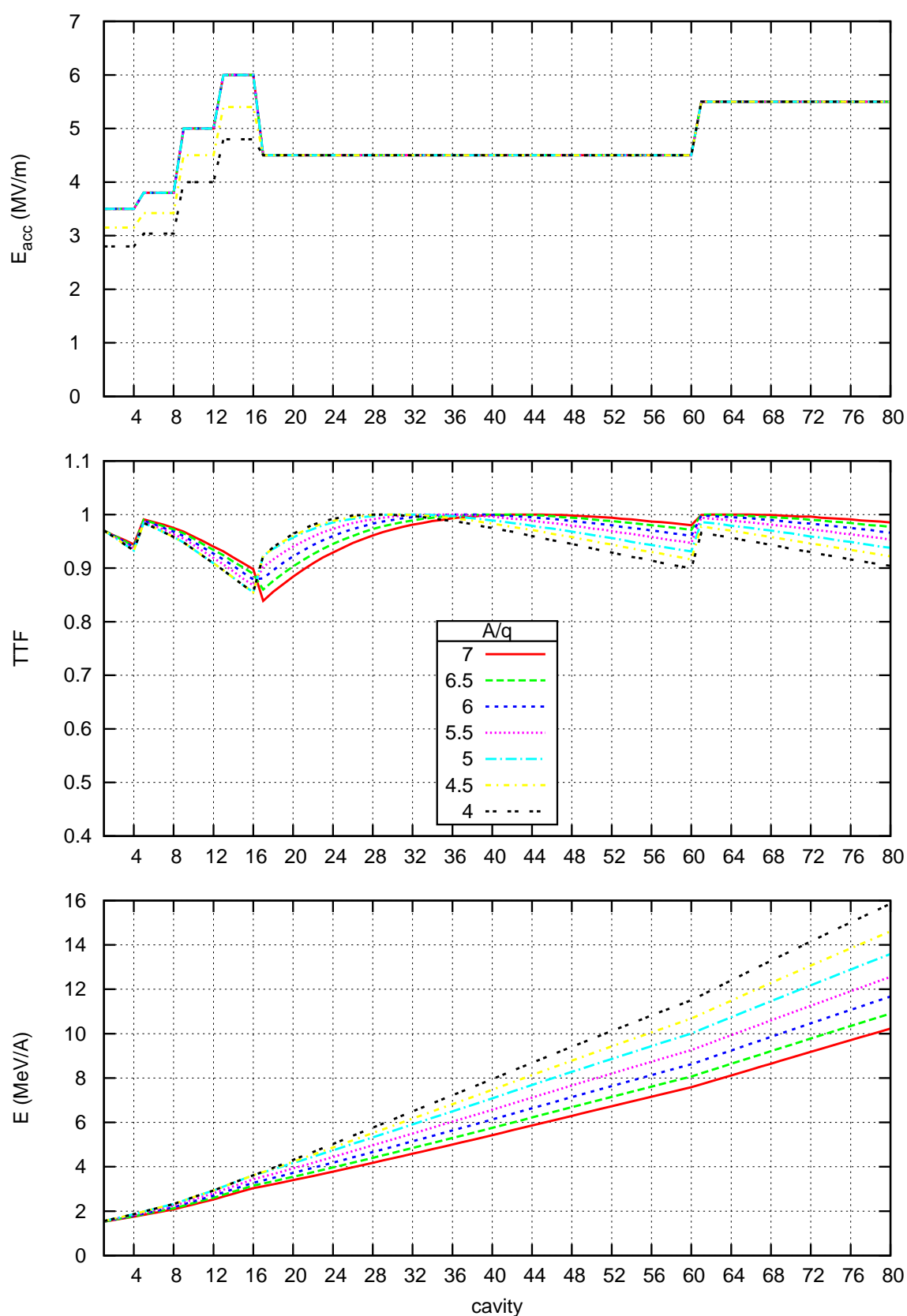


Figure 5.10: Performances of ALPI for SPES scenario. Option II, high-beta branch upgrade.

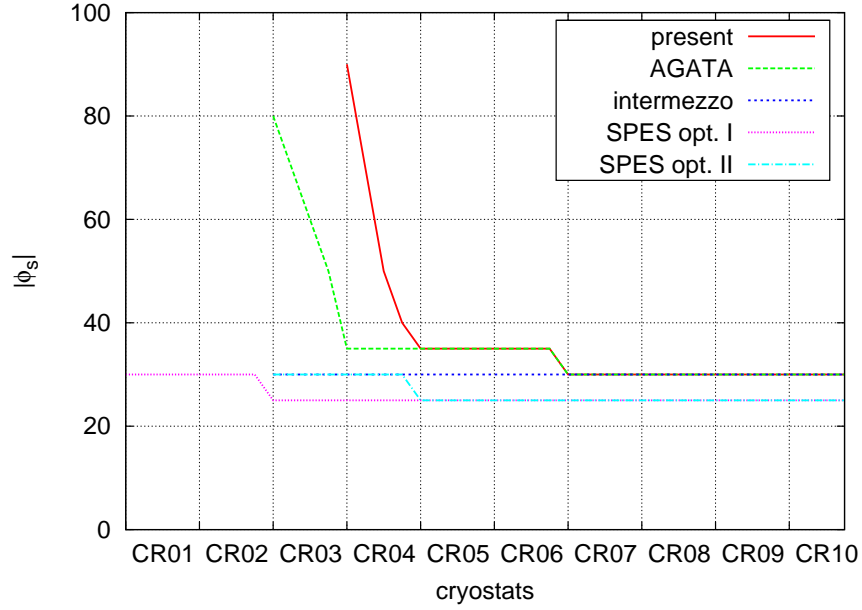


Figure 5.11: Synch. phase absolute value along the low-energy branch for the different scenarios.

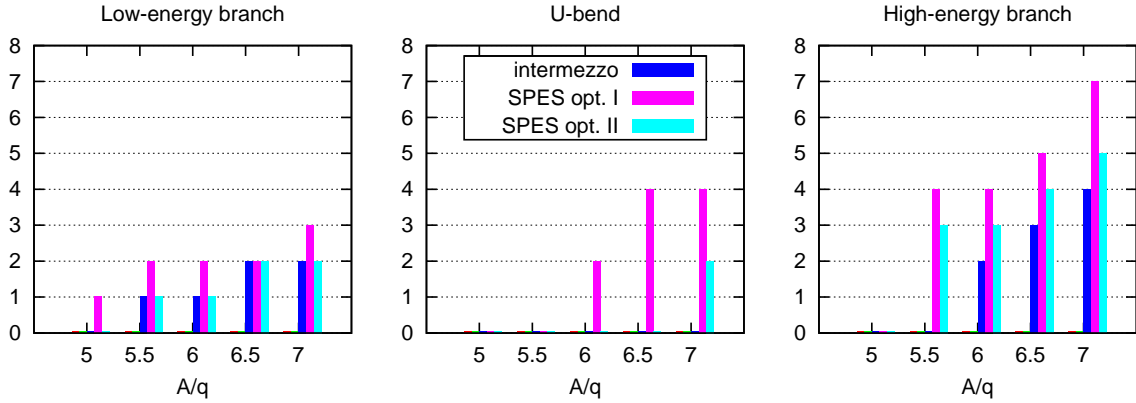


Figure 5.12: Number of magnets out of specifications for the different scenarios.

## 5.5 Comparison between the scenarios

Figure 5.13 summarizes the performances of the different scenarios. The Equivalent Voltage is here defined as the energy gain of the beam divided by the charge and the efficiency is the Equivalent Voltage divided by the total accelerator voltage.

The best performing scenario is SPES Option II: even if the total voltage is higher for SPES Option I, the better efficiency gives higher final energies as a result. Concerning the number of magnets out of specs, this scenario saves one magnet in the low-energy and two in the high-energy branch (see Fig. 5.12). Those two more magnets of the U-bend to be replaced for Opt. II are not counted because they can be replaced by two of the discarded high-energy triplets.

Figure. 5.11 shows the use of the synchronous phases along ALPI low-energy branch. From this graph it is clear how the "funnel" bunching works when a dedicated buncher is missing. When the buncher is present, from "intermezzo" scenario on, it is possible to use a lower  $|\phi|$ . For the two SPES scenarios a big advantage is the lower longitudinal emittance obtained with the new PIAVE design and therefore an even narrower acceptance can be used safely.

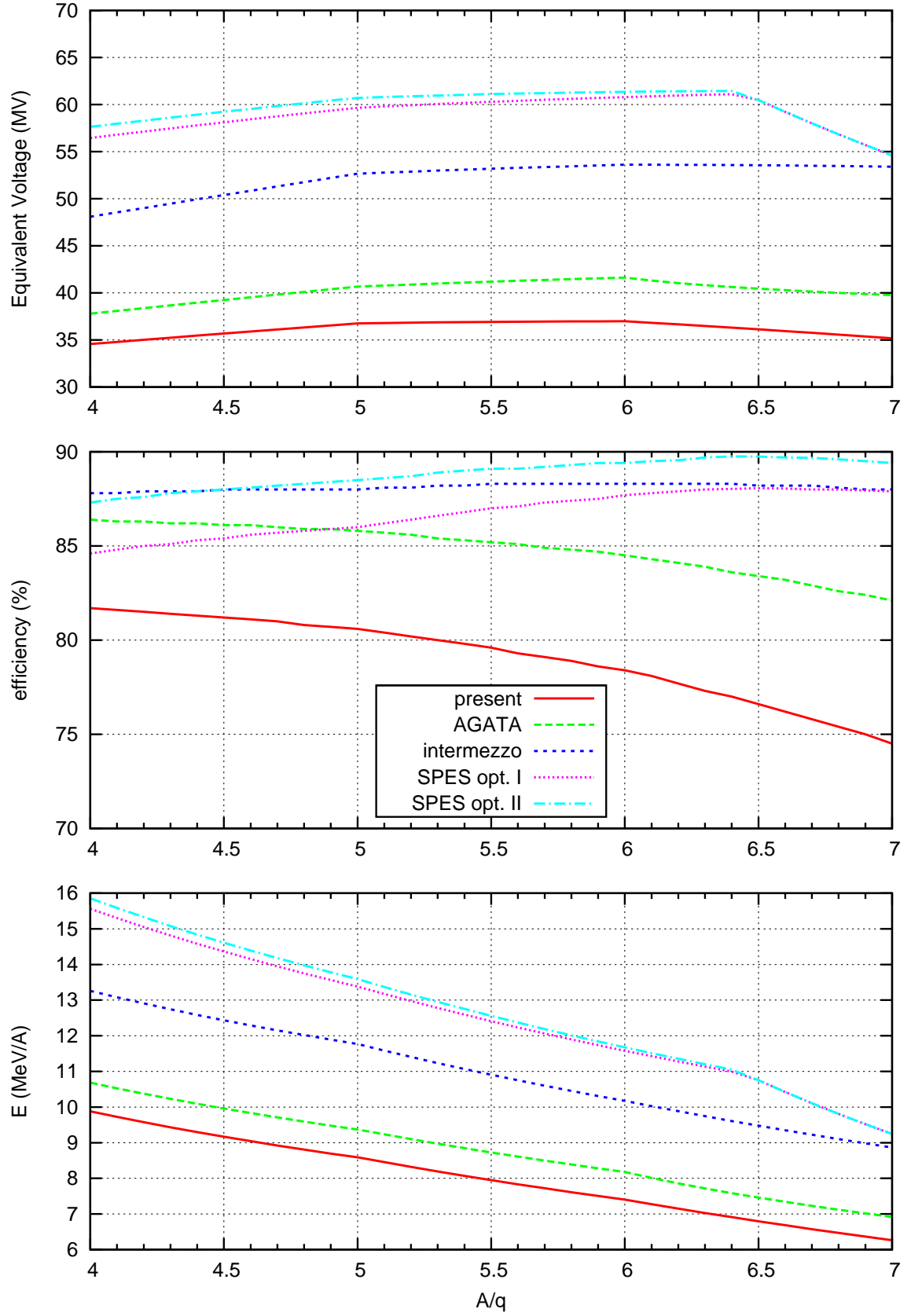


Figure 5.13: ALPI upgrade scenarios performances. The colored lines represent the different upgrade scenarios. SPES scenarios are limited by the maximum rigidity inside the dipole (3.0 T·m).

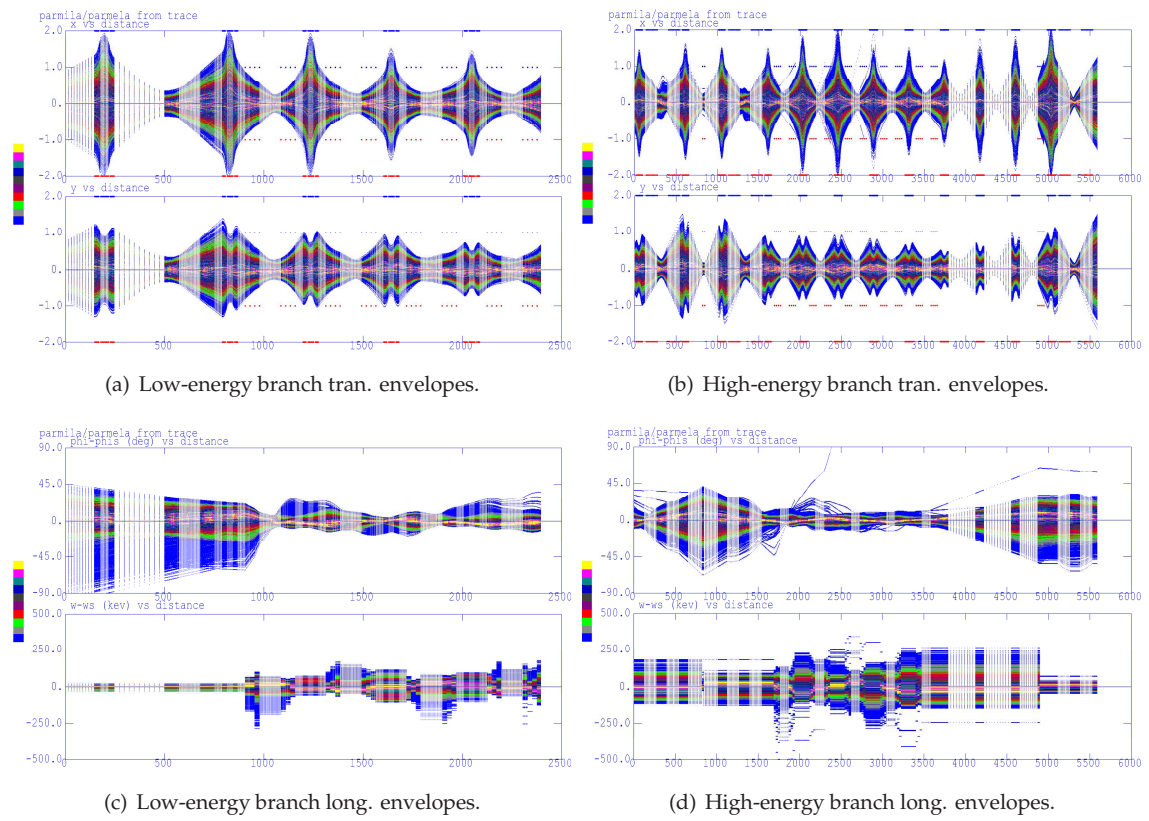
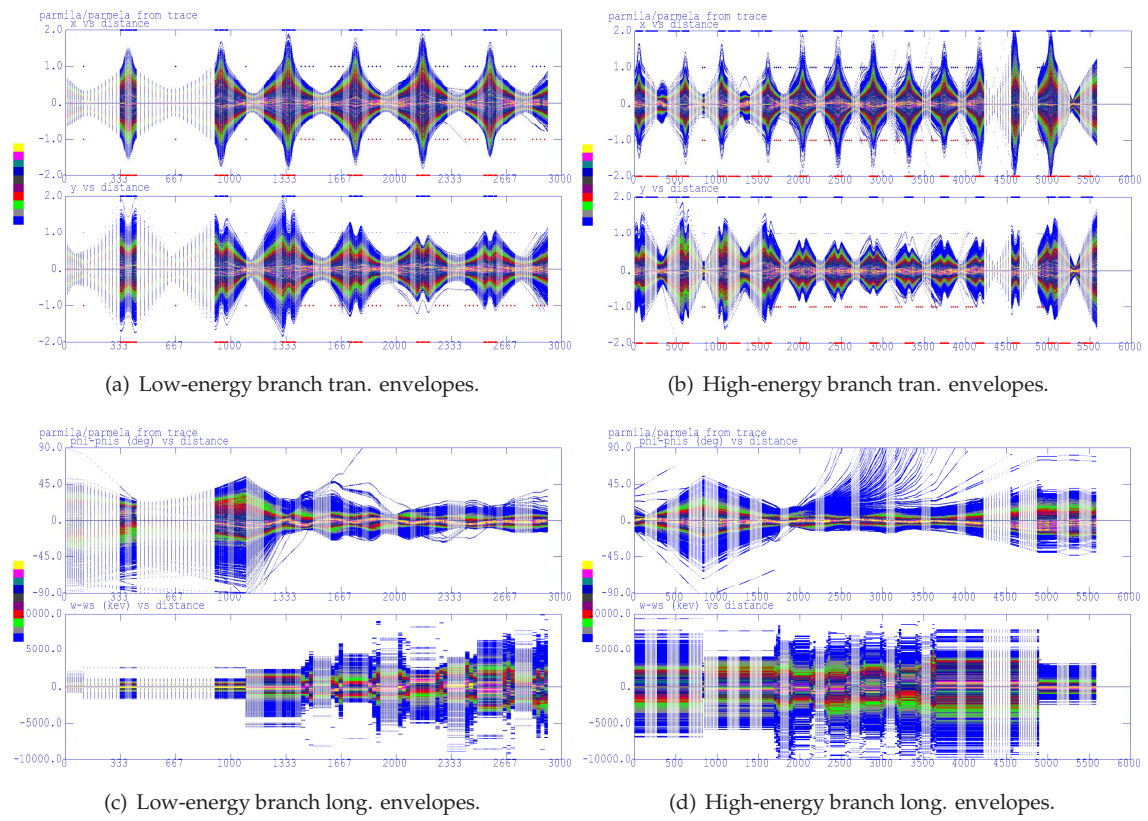


Figure 5.14: AGATA scenario. PARMELA simulation for  $A/q = 7$ .



Figure 5.15: Scenario "intermezzo". PARMELA simulation for  $A/q = 7$ .

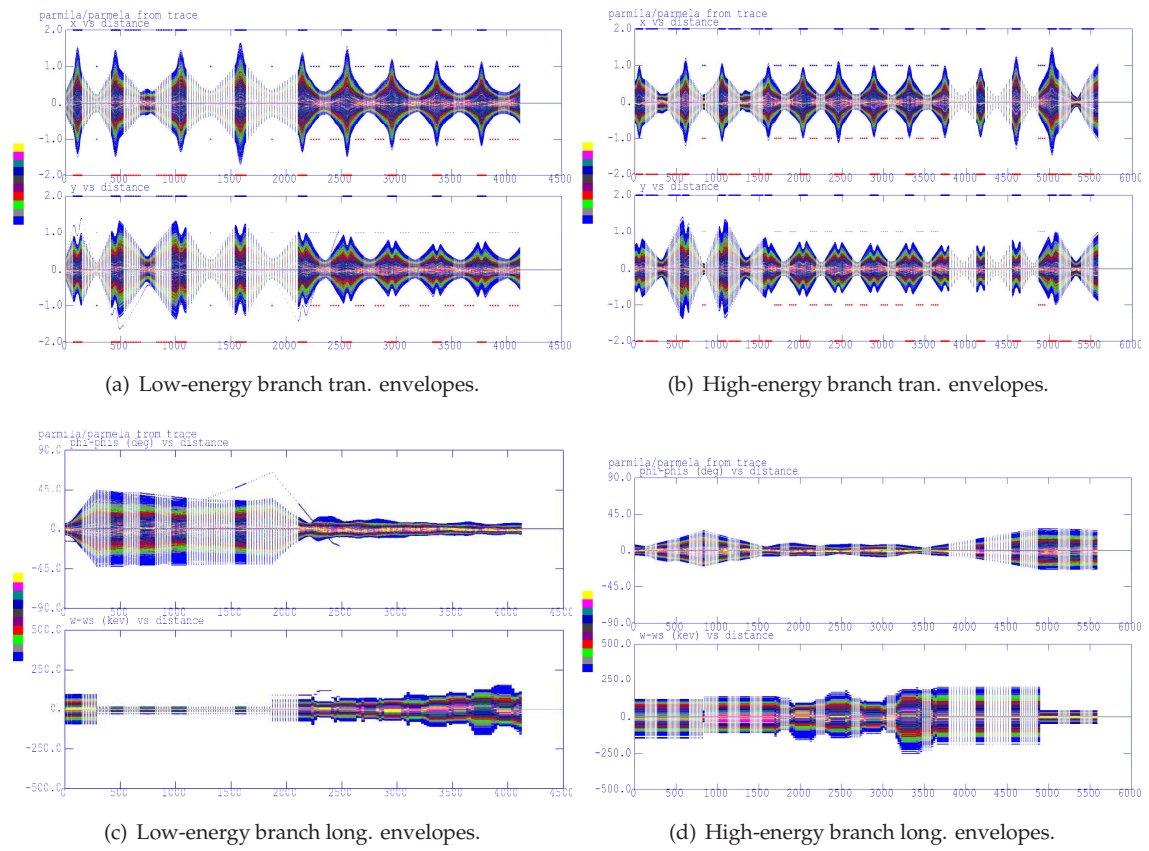
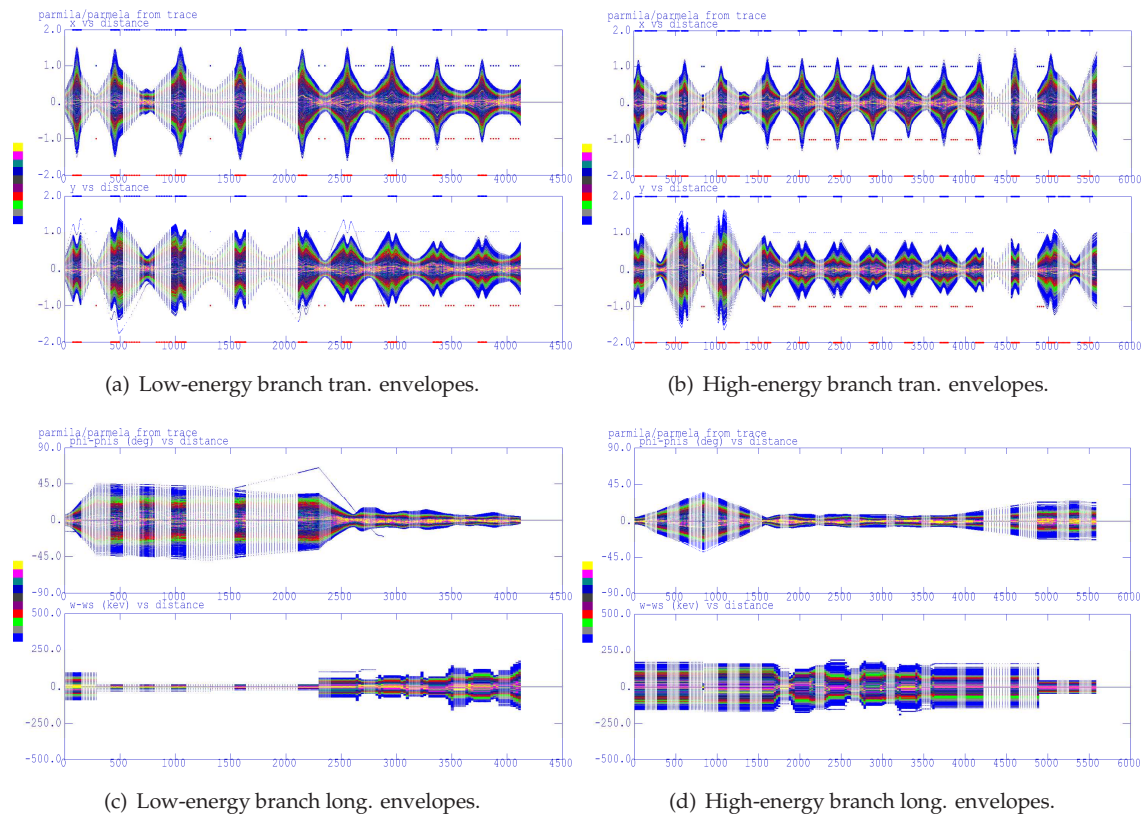


Figure 5.16: SPES Opt. I scenario. PARMELA simulation for  $A/q = 7$ .

Figure 5.17: SPES Opt. II scenario. PARMELA simulation for  $A/q = 7$ .

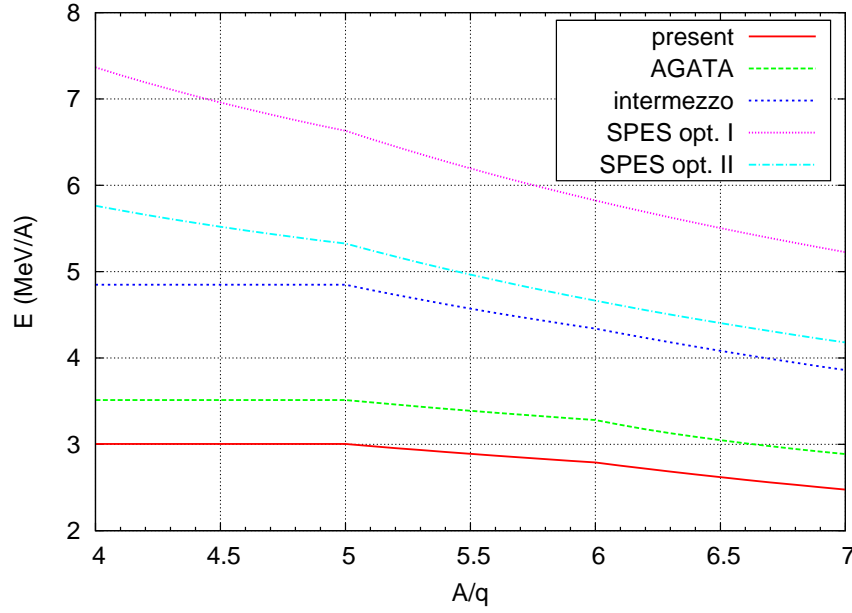


Figure 5.18: Energy at stripper station for the different scenarios.

## 5.6 The stripper option

As described in Chapter 4, the solution of using a stripper foil in the middle of the acceleration allows to reach higher energies with lower beam rigidity, that is a less demanding solution from the magnets point of view.

The upgrades not only offer higher final energies depending on the scenario, but also give the chance of having higher energies at the stripper station (see Fig. 5.18). Higher is the energy at the stripper station, higher is the average charge after stripping and higher is the final energy if the same voltage is applied. The situation is more complicated by the fact that the different upgrade scenarios foresee also different total voltages of ALPI high-energy branch.

The results of the calculations which take into account all these parameters are described in Fig. 5.19: combining the energy at the stripper station as function of  $A/q$ , the LEGIS charge states as function of  $A$  (Eq. 3.6) and the valley of nuclear stability parametrization of Eq. A.6, it is possible to get charge state after stripping, the probability of the most probable charge state and the final energy as function of  $Z$ .

The best performing scenario once the stripping is used is SPES Option II, but the scenario "intermezzo" shows performances which already satisfy the nuclear community. Even if it is possible to see from Fig. 5.14, 5.15, 5.16 and 5.17 that the beam is always focalized in the center of the last low-energy period, the drawback of "intermezzo" is that the present PIAVE injector has poorer emittance performances and the losses are certainly greater than for any SPES scenario.

The beam rigidity is such that no new magnets are required for the U-bend and the high-energy branch for any upgrade scenario if the stripper is used and no limitations come from the dipoles maximum field.

It is important to remark that the stripper option gives higher energies at the cost of a much lower transmission: currents on target of the order of 1 pA are guaranteed, but for some experiments both for AGATA and SPES this value is not sufficient.

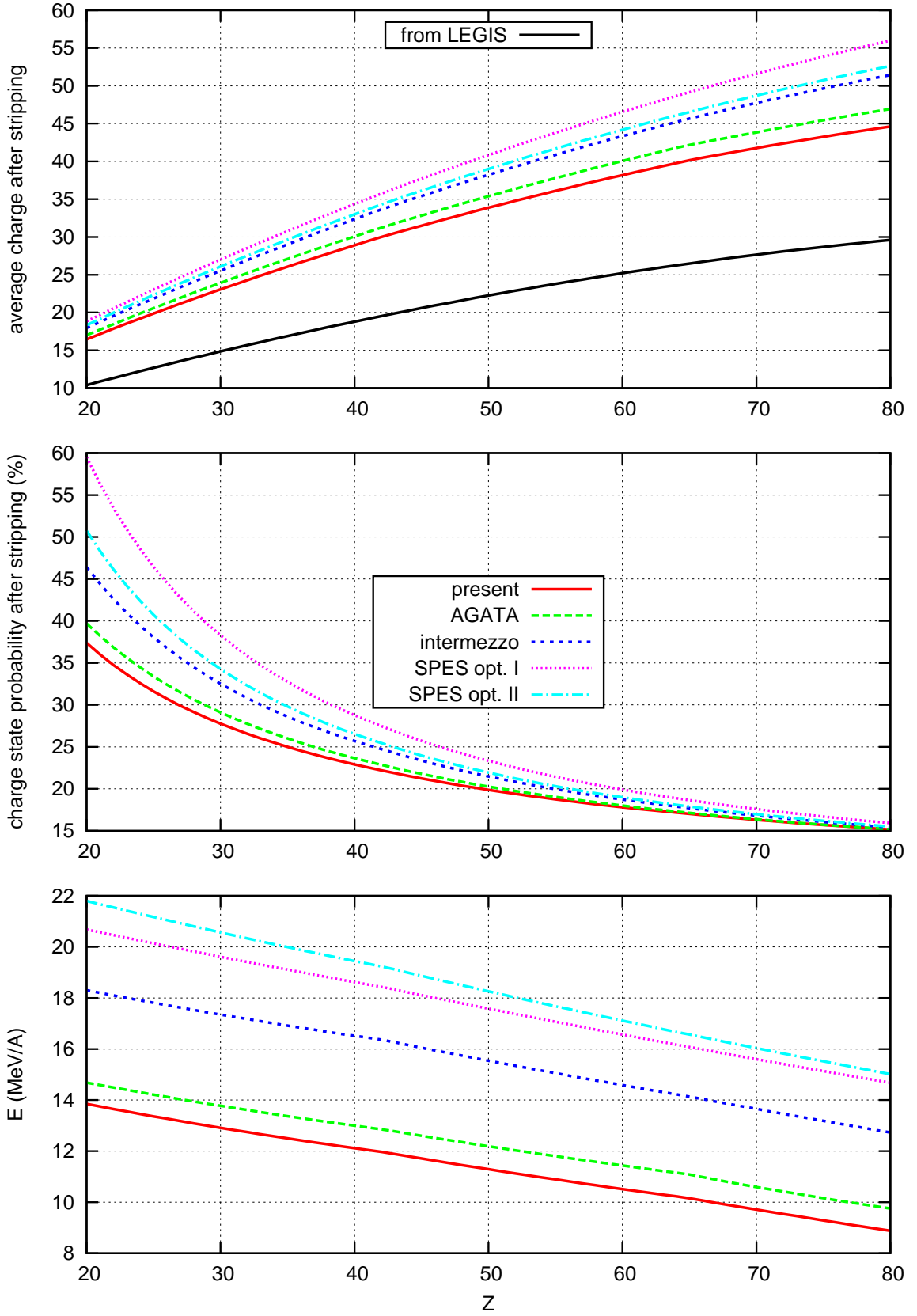


Figure 5.19: ALPI upgrade scenarios performances using the stripper. The LEGIS charge state curve comes from Eq. 3.6 and the charge after stripping from the average of Eq. 4.7 and Eq. 4.8.

## Bibliography

- [1] D. Zenere, A. Facco, and F. Scarpa, "Progress in the ALPI-PIAVE low-beta section upgrade," in *Proceedings of EPAC08*, (Genoa, Italy), pp. 3413–3415, 2008.
- [2] S. Stark, A. M. Porcellato, and al., "Progress in the ALPI-PIAVE low-beta section upgrade," in *Proceedings of the 13th International Workshop on RF Superconductivity*, (Peking, China), 2007.
- [3] P. N. Ostroumov and K. W. Shepard, "Correction of beam-steering effects in low-velocity superconducting quarter-wave cavities," *Phys. Rev. ST Accel. Beams*, vol. 4, p. 110101, Nov 2001.
- [4] R. E. Laxdal and al., "Cryogenic, magnetic and RF performance of the ISAC-II medium beta cryomodule at TRIUMF," in *Proceedings of PAC05*, (Knoxville (TN), USA), pp. 3191–3193, 2005.
- [5] A. Facco, "Private communication."
- [6] P. Modanese and al., "Upgrading of ALPI-LINAC cryogenic transfer lines," in *LNL Annual Report 2006*, (Legnaro, Italy), INFN, 2006.